substance: $CrSi_2$-type ternary alloys
property: physical properties

$Cr_{1-x}M_xSi_2$ homogeneity ranges

Ti:	$x \leq 0.9$ at 1570 K [58P]
Zr:	$x \approx 0$ at 1570 K [58P]
V:	$x = 0...1$ [62W]
Ta:	$x \leq 0.12$at 1570 K[58P]
Mo:	$x < 0.3$ at 1570 K [58P, 65N]
W:	$x \leq 0.15$ at 1570 K [58P]
Mn:	$x \leq 0.225$ [78N, 62W]
Re:	$x \leq 0.1$ at room temperature [65N]
Fe:	$x \leq 0.01$ [62W]
Co:	$x \leq 0.02$ [71N], $x \approx 0$ [62W]
Ni:	$x \approx 0$ [62W].

$Cr_{1-x}V_xSi_2$: non-metallic limit x = 0.1 [63S]. RT values of electrical conductivity $1/\rho$ and Seebeck coefficient S: Fig. 10.

$Cr_{1-x}Mo_xSi_2$, $Cr_{1-x}W_xSi_2$: resistivity ρ and thermoelectric power S decrease with increasing x. Semiconductor properties of $Cr_{0.9}Mo_{0.1}Si_2$ ($Cr_{0.25}Mo_{0.1}Si_{0.65}$?) deduced from $\rho(T)$ and $S(T)$ up to ≈ 1800 K [70T].

$Cr_{1-x}Mn_xSi_2$: resistivity ρ: Figs. 1, 2, 10; Hall effect: Figs. 3, 4; Seebeck coefficient S: Figs. 5, 6, 10; mobility: Figs. 7, 8; carrier concentration: Fig. 9.

References:

58P Pearson, W. B.: "A Handbook of Lattice Spacings and Structures of Metals and Alloys". Vol. 1, Pergamon Press 1958, reprinted 1964.

62W Wittmann, A., Burger, K. O., Nowotny, H.: Monatsh. Chem. 93 (1962) 674.

63S Sakata, T., Tokushima, T.: Trans. Ntl. Res. Inst. Met. 5 (1963) 34.

64S Shinoda, D., Asanabe, S., Sasaki, Y.: J. Phys. Soc. Jpn. 19 (1964) 269.

65N Neshpor, V. S., Samsonov, G. V.: Izv. Akad. Nauk SSSR, Neorg. Mater. 1 (1965) 665 (translation: Inorg. Mater. 1 (1965) 599).

70T Terekhov, G. I., Tagirova, R. Kh., Ivanov, O. S.: Izv. Akad. Nauk SSSR, Metal. (1970) 177 (translation: Russian Metallurgy (1970) 126).

71N Nikitin, F. N., Tarasov, V. I.: Fiz. Tverd. Tela 13 (1971) 3473 (translation: Sov. Phys. Solid State 13 (1972) 2938).

73N Nikitin, F. N., Tarasov, V. I., Zaitsev, V. K.: Fiz. Tverd. Tela 15 (1973) 1254 (translation: Sov. Phys. Solid State 15 (1973) 846).

78N Nishida, I., Sakata, T.: J. Phys. Chem. Solids 39 (1978) 499.

Fig. 1.

$CrSi_{2+\delta}$ and $Cr_{0.88}Mn_{0.12}Si_2$. Resistivity vs. reciprocal temperature [64S]. *1*: $CrSi_2$ (single crystal of unknown orientation), *2*: $CrSi_{2.01}$ (polycrystalline), *3*: $CrSi_{2.02}$ (polycrystalline), *4*: $Cr_{0.88}$ $Mn_{0.12}Si_2$ (crystal grown by the Bridgman technique).

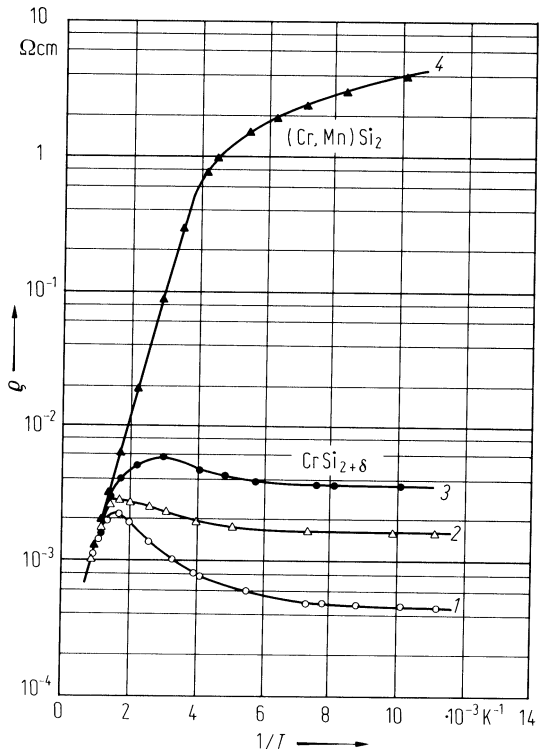

Fig. 2.

$Cr_{1-x}Mn_xSi_2$. Resistivity vs. reciprocal temperature for hot-pressed samples annealed at 1373 K [78N]. Mn concentration (in parentheses) in 10^{21} cm^{-3}. *1*: x = 0, *2*: x = 0.059 (1.65), *3*: x = 0.100 (2.80), *4*: x = 0.115 (3.23), *5*: x = 0.142 (3.99), *6*: x = 0.182 (5.12).

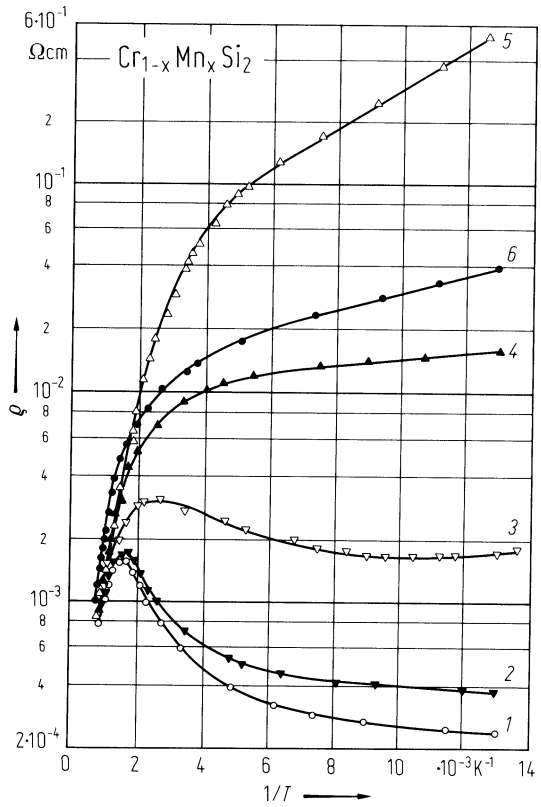

Fig. 3.

$CrSi_{2+\delta}$ and $Cr_{0.88}Mn_{0.12}Si_2$. Hall coefficient vs. reciprocal temperature [64S]. Symbols as in Fig. 1.

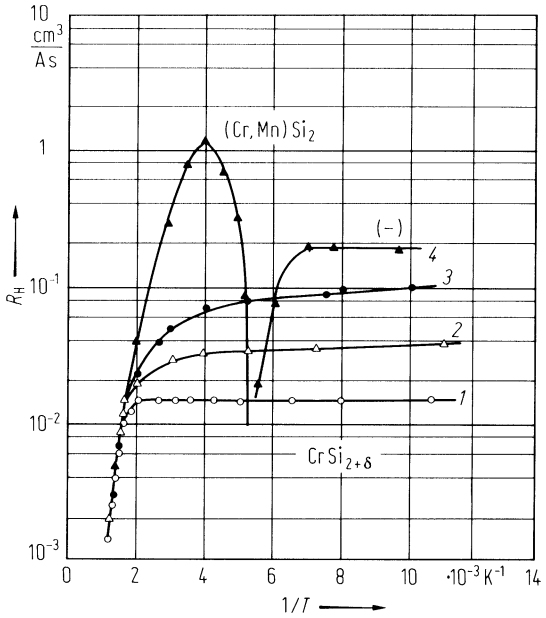

Fig. 4.

$Cr_{1-x}Mn_xSi_2$. Hall coefficient vs. reciprocal temperature [78N]. Mn concentrations as in Fig. 2.

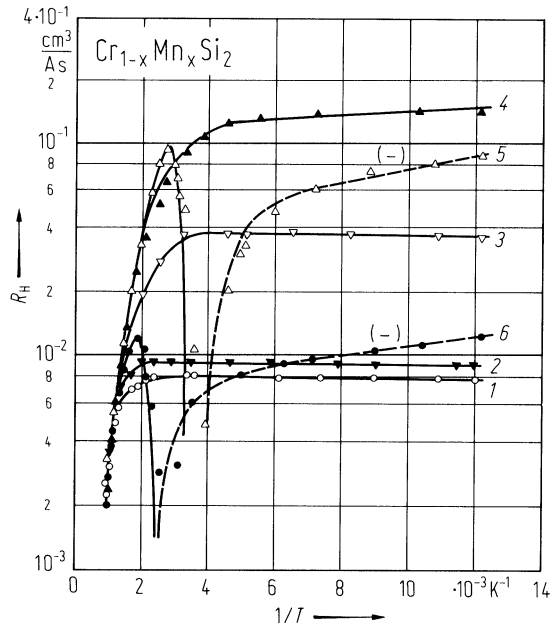

Fig. 5.

$CrSi_{2+\delta}$ and $Cr_{0.88}Mn_{0.12}Si_2$Thermoelectric power vs. temperature [64S]. The solid curves are calculated. Symbols as in Fig.1.

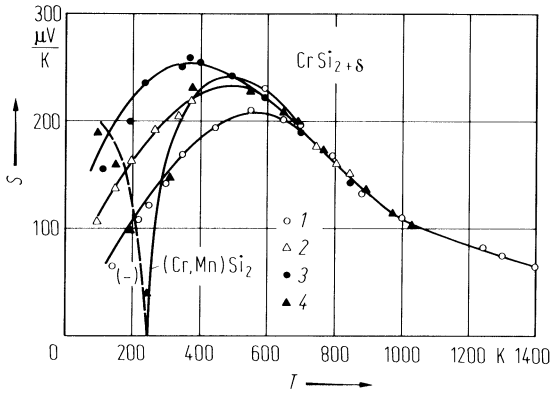

Fig. 6.

$Cr_{1-x}Mn_xSi_2$. Seebeck coefficient *S* vs. temperature [78N]. Mn concentrations as in Fig. 2. Solid and dashed curves are calculated for acoustic lattice scattering and for impurity ion scattering, respectively.

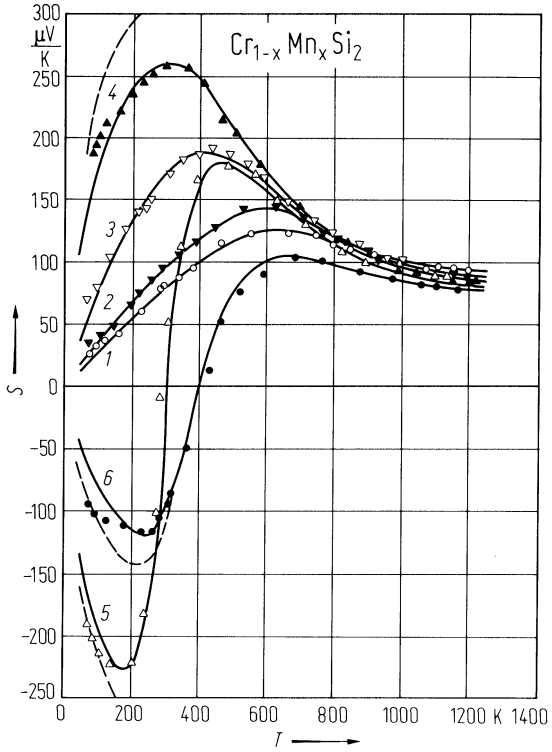

Fig. 7.

$CrSi_{2+\delta}$ and $Cr_{0.88}Mn_{0.12}Si_2$. Hall mobility of holes vs. temperature in a doubly-logarithmic scale [64S]. Symbols as in Fig. 1.

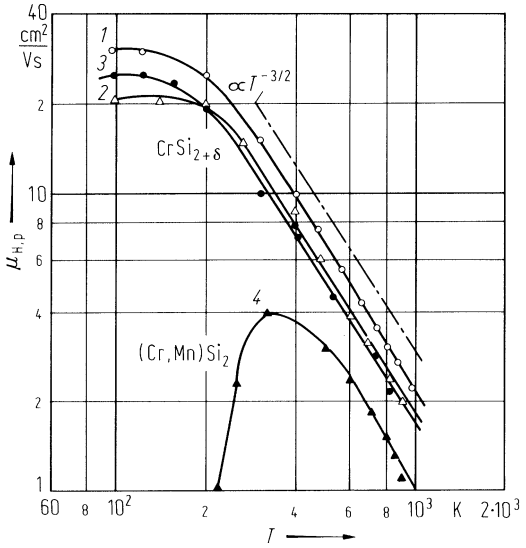

Fig. 8.

$Cr_{1-x}Mn_xSi_2$. Hall mobilities vs. reciprocal temperature in a doubly-logarithmic scale [78N]. Mn concentrations as in Fig. 2. Samples are hot-pressed at 1473 K and annealed at 1373 K.

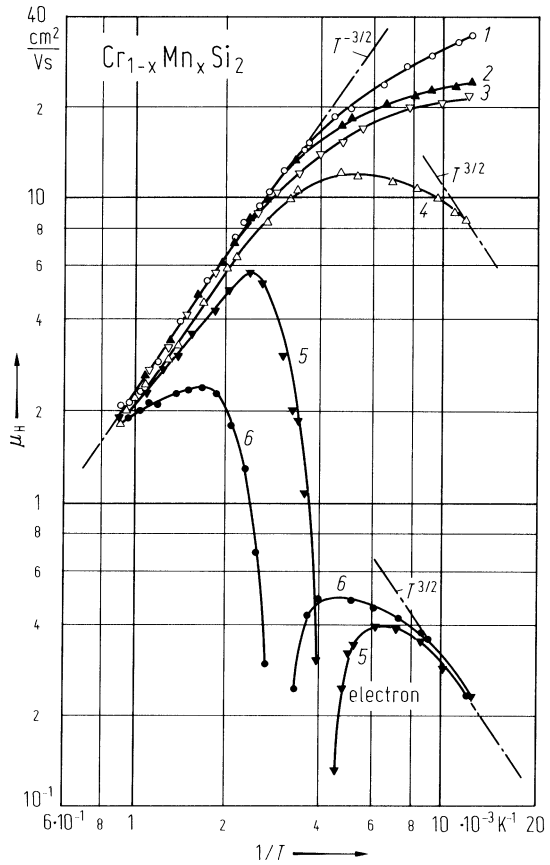

Fig. 9.

$Cr_{1-x}Mn_xSi_2$. Carrier concentrations vs. reciprocal temperature [78N]. Mn concentrations as in Fig. 2. Curves *1*, *2*, *3*, *4*: holes; *5*, *6*: electrons.

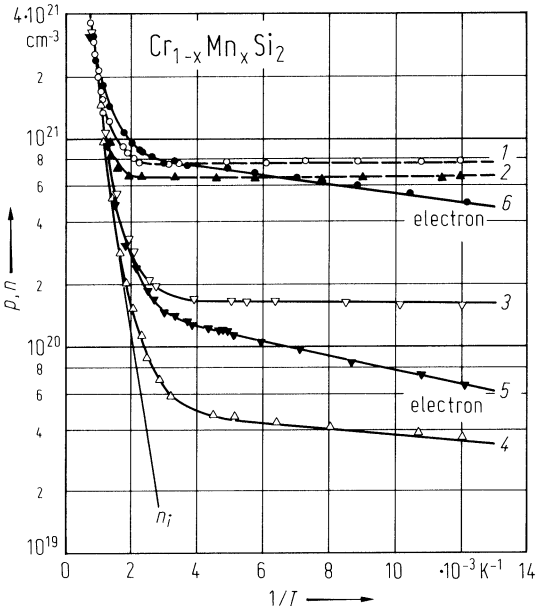

Fig. 10.

$Cr_{1-x}V_xSi_2$ and $Cr_{1-x}Mn_xSi_2$. Electrical conductivity σ and thermoelectric power S vs. concentration [73N]. T = 295 K, polycrystalline samples.